Optical Antennas in Hybrid Photonic Systems

Ruud Hendrikx, Hugo Doeleman, Freek Ruesink, A. Femius Koenderink, and Ewold Verhagen*
Center for Nanophotonics
FOM Institute AMOLF
1098 XG Amsterdam, The Netherlands
*verhagen@amolf.nl

***Abstract*— Plasmonic nano-antennas are widely employed for sensing and enhancing light-matter interactions. They are characterized by deeply subwavelength optical mode volumes as well as broad resonance linewidths. By coupling nano-antennas to resonant modes of dielectric photonic cavities, which have a larger mode volumes in combination with very high-*Q* resonances, a hybrid system is created with eigenmodes that combine the traits of the individual constituents in a highly versatile fashion. The resulting systems are suitable to achieve strong field enhancements over a tunable bandwidth. We study the properties of the resulting eigenmodes of the coupled system, and show how they can be used for both efficient excitation as well as extraction of radiation. We experimentally realize a system consisting of nano-antennas coupled to a silica whispering gallery mode resonator. We show how this can be used to quantify the change of the antenna polarizability related to the alteration of the local density of states by the nearby microcavity mode. Moreover, we study the eigenmodes of the hybrid system in terms of their spectral and radiation properties. We observe pronounced alterations of the cavity frequency and linewidth when it is perturbed by nano-antennas, and systematically investigate the dependence of those shifts on the properties of the nano-antennas.**

Keywords—optical antennas; microcavities; radiative effects

I. Introduction

Enhancing local electromagnetic fields through making use of resonant modes is at the basis of applications ranging from radio to optical frequencies. In fact, many concepts to create resonant optical systems can be ported between very different frequency regimes. At optical frequencies, resonant field enhancement is used for several important purposes related to enhancing light-matter interactions, including optical sensing and spectroscopy of small concentrations of molecules and enhancing spontaneous emission through an enhanced local density of optical states, known as the Purcell effect. Two approaches find wide application: On the one hand, high-quality micro- or nanocavities are used, including Fabry-Pérot etalons, whispering gallery mode resonators, and photonic crystal defect cavities [1]. On the other hand, optical antennas, consisting of suitably shaped metallic nanostructures with plasmonic resonances that are strongly coupled to radiation, are employed to create strong fields in localized hotspots [2]. The two approaches both rely on storing light in a confined volume V for an appreciable time, as expressed by the resonance quality factor Q. The Purcell factor, and likewise the possible field enhancement, scales with the ratio Q/V [3]. The two approaches reach high Q/V ratios in very different ways: whereas micro- and nanocavities can exhibit quality factors regularly exceeding 10^5 and even reaching 10^9, their mode volumes are typically at least one to hundreds of μm cubed [1]. In contrast, nano-antennas exhibit strong optical loss due to absorption (Ohmic heating) or radiation, leading to $Q \approx 10$, whereas their nanoscale field confinement means effective mode volumes can be deeply subwavelength.

We propose to use hybrid systems, comprising coupled high-Q microcavity resonances and optical nano-antennas, as a platform for enhancing light-matter interactions [4-7]. The coupling is established by placing a radiating plasmonic nano-antenna in the modal field of a microcavity. This approach yields a highly flexible system, the properties of which can be tailored to strike the balance between quality factor and mode volume that is most suitable to an application. Indeed, whereas high-Q cavities can show excellent field enhancement, their narrow linewidths often make them impractical for applications, due to the challenge to interface narrow-band sources with the systems, or integrate many systems together. By coupling them to nano-antennas, the bandwidth of their cavity modes can be increased, while still obtaining high enhancements Q/V at the places of maximum field, close to the nano-antenna.

In this work, we present a model system, consisting of a glass microsphere supporting high-Q whispering gallery modes, evanescently coupled to arrays of Au nanorods supporting localized plasmonic antenna resonances. We aim to characterize the optical modes of the hybrid system. In particular, we investigate the influence of the nanorods on the cavity mode frequency and linewidth. We demonstrate pronounced perturbation of the optical cavity, as evident from cavity transmission spectra. We observe both increase and decrease of the cavity linewidth upon introducing the nano-antennas in the cavity near field, depending on the spatial profile of the cavity mode. This is related to constructive and destructive interference, respectively, of the radiation scattered by the antennas with direct leakage radiation from the cavity.

II. Methods

Silica microsphere resonators are fabricated by CO_2 laser melting of the cleaved end of a standard SMF-28 optical fiber. Through a controlled laser reflow process, microspheres (diameter 50-120 μm) are fabricated at the end of the fiber [8],

This work is part of the research programme of the Foundation for Fundamental Research on Matter (FOM), which is financially supported by the Netherlands Organisation for Scientific Research (NWO). E.V. gratefully acknowledges support from an NWO-VIDI grant.

which acts as mechanical support (see Fig. 1a). The spheres support optical whispering gallery modes from the visible to the near-IR regime with quality factors up to ~10^8 [9]. The sphere support is glued to a 3-axis piezo-stage, which allows positioning the microcavity close to a vertically mounted glass cover slide on which arrays of gold nano-antennas are defined. The antennas are fabricated using e-beam lithography followed by vacuum evaporation of 40 nm Au and liftoff. The Au nanorods are 125 nm wide and 400 nm long, and placed in a rectangular array with pitches of 800 and 900 nm (see Fig. 1b). Separate far-field transmission measurements (not shown) reveal that these antennas support strong plasmonic resonances with a Q of ~10 close to a free-space resonance wavelength of 1500 nm, which can be associated with dipole modes polarized along the antenna's long axis [10].

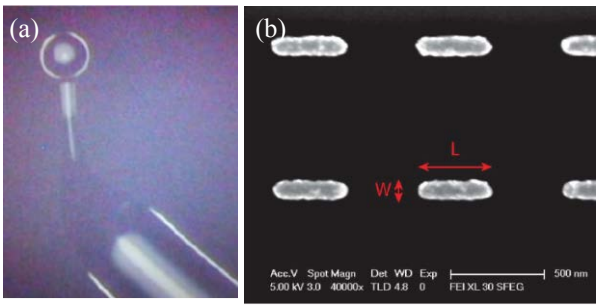

Fig. 1. (a) Optical micrograph of fabricated high-Q microsphere. The diameter of the sphere is 60 µm. (b) SEM image of gold nano-antennas, fabricated in an array on a glass substrate.

As sketched in Fig. 2a, the antenna arrays are placed in the near field of the microcavity, at controllable distance (down to a minimum separation of typically ~1 µm). As the field of the whispering gallery modes extends in the air just outside the sphere (with evanescent $1/e$ intensity decay length of ~200 nm), this establishes a coupling between microcavity and antennas, with a strength that is controllable through their separation. The antennas are oriented such that their long axis is aligned to the electric field of the considered TE-polarized cavity modes. A tapered optical fiber (waist diameter ~1 µm) is brought close to the microsphere from the other side of the sphere using a second piezo stage. It serves to couple light in and out of the sphere with high efficiency through wave-vector-matched evanescent coupling [11].

By monitoring the transmission of a narrowband tunable diode laser (New Focus TLB-6728, ~1550 nm) through the tapered fiber, spectra can be obtained that reveal the frequency and linewidth of the modes of the cavity. Figure 3 shows a transmission spectrum for exactly one free spectral range of the cavity, in absence of the substrate with nano-antennas. Many modes are visible, grouped in several 'mode families'. The different families correspond to modes with different radial dependence, whereas their members correspond to modes with different polar field dependencies, indicated by integer l. For a perfect sphere, these modes would be degenerate for each azimuthal mode number m [12]. However, due to slight ellipticity of our microspheres (which can be controlled during the reflow process), the degeneracy is lifted and modes with different numbers of field nodes l-m along the polar direction can be individually addressed. These modes with different polar mode numbers can be clearly recognized by monitoring the radiation leaking into the substrate, that is collected with a high-NA objective (Fig. 2). In Fig. 3 images of that leakage radiation is shown for the three lowest-order polar modes. The microscope is focused on the substrate surface, and both images of that surface ('real space') as well as of the back focal plane of the objective ('momentum space') are shown, to show the spatial and angular dependence of the radiation.

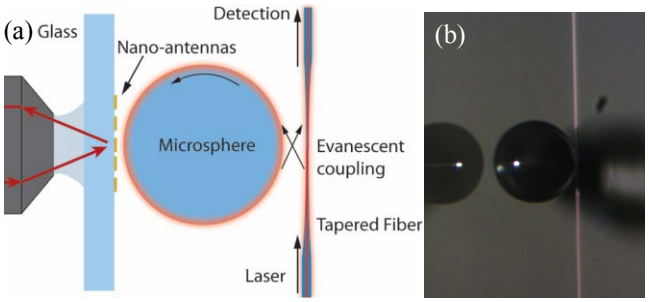

Fig. 2. Experimental setup: (a) schematic, (b) optical micrograph (top view). The microsphere is visible, with on the right the tapered optical fiber for in- and outcoupling. The second sphere visible on the left is a reflection in the glass substrate carrying the nano-antennas (mounted out of plane).

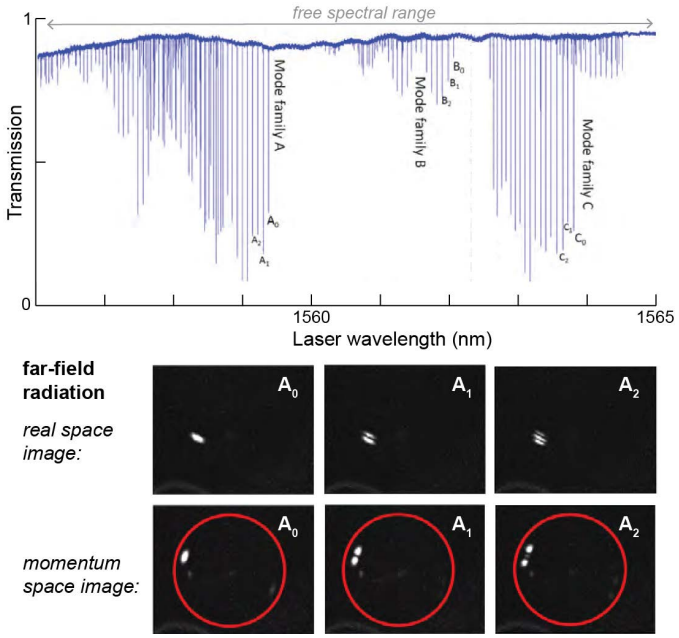

Fig. 3. (top) Cavity spectroscopy (transmission vs laser wavelength) spanning one free spectral range. Within each mode family, the rightmost (largest wavelength) resonance corresponds to the lowest value of l-m. (bottom) For the three lowest-order modes labeled 'A0'-'A2', images of cavity radiation collected through the high-NA objective (see Fig. 2, NA=1.49) are shown. The top row shows images of the plane of the cavity surface, revealing small areas (length ~5 µm) from which radiation originates, where the cavity mode is brought close to the glass substrate. The bottom row shows images of the back focal plane (indicated by red circle), highlighting the different angular distributions of the emission of the three modes.

III. Results: Cavity perturbation

The transmission spectrum around one such mode (in this case, with a large, undetermined polar mode number *l*-*m*) is plotted in Fig. 4, as a function of the frequency detuning Δ_0 from the (unperturbed) mode resonance frequency. From bottom to top, the different spectra are taken for decreasing separations between the cavity and the glass substrate, shifted for clarity. Figure 4a shows the effect of the bare substrate approaching, which serves as a reference measurement without the antennas. Figure 4b shows the effect of a field of nano-antennas, taken for the same set of distances as panel a. Both show a pronounced broadening as the substrate is approached, but to a different extent for the sample with nano-antennas, which moreover shows a strong frequency shift of the cavity resonance [13,14].

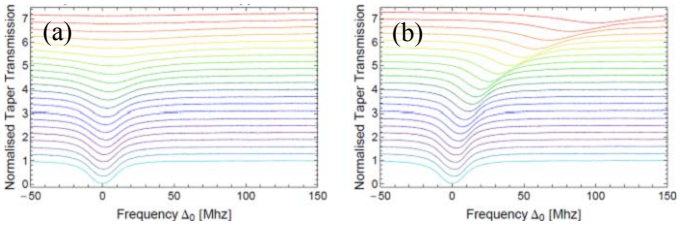

Fig. 4 (a) Cavity transmission spectra around one of the cavity resonances, for various separations between the microsphere and the glass substrate. (b) Spectra for the same microsphere resonance, for various separations to an antenna-covered substrate.

The resonance frequency change ('lineshift', $\delta\omega$) and linewidth (κ), obtained from fits to the spectra in Fig. 4, are plotted in Fig. 5 as a function of cavity position. The effect of the antenna array (red) is compared to that of the bare glass substrate (blue). Two reference measurements are taken at opposite sides of the antenna array, in order to verify that the measurements are taken at comparable distances. As can be seen, the frequency shift due to the antennas is much stronger than that due to the glass as it enters in the cavity mode volume. Moreover, the antennas lead to a strong *reduction* of the cavity linewidth, as compared to the substrate without the antennas.

Apparently, even though the antennas are strong scatterers and are as such expected to lead to strong scattering of the cavity to free-space loss channels, this does not mean that the total cavity loss rate is increased. Instead, when compared to the case without the antennas (but with the glass substrate present), the cavity radiation is reduced. This is possible when the antenna-induced scattering interferes destructively with the intrinsic radiation of the cavity [15,16,17]. Indeed, as the cavity approaches the bare glass substrate, the linewidth is dominated by direct radiation in the glass, enabled because of wave-vector matching of the cavity mode to plane waves in the glass substrate escaping at a well-defined angle. This radiation will interfere with that of the antennas, which act as a phased array to emit at (approximately) the same angle. Destructive interference in the far field limits the total radiated power, and therefore reduces the linewidth of the hybrid cavity-antenna mode with respect to that of the cavity alone.

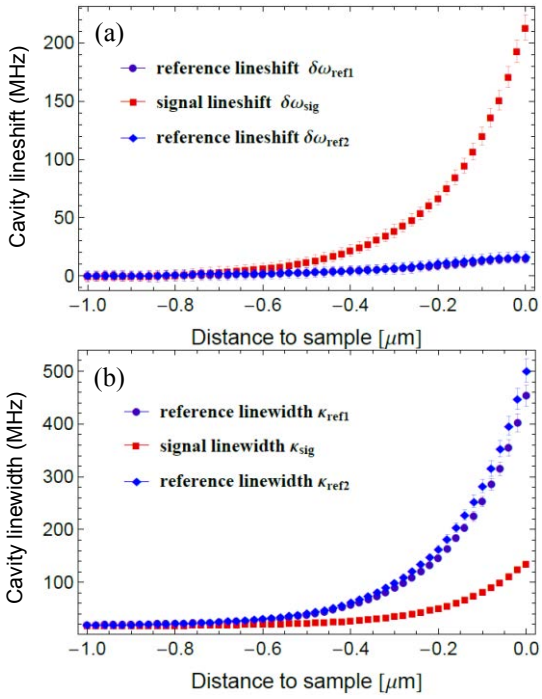

Fig. 5. Cavity resonance frequency (a) and linewidth (b) as a function of cavity-substrate separation, for a bare substrate (blue, 'reference') and one coated with nano-antennas (red, 'signal').

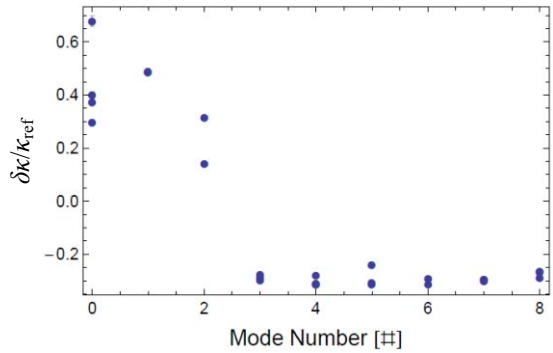

Fig. 6. Relative antenna-induced linewidth change (normalized to the linewidth $\kappa_{(sub)}$ on the bare substrate at the same separation), as a function of polar mode number (*l*-*m*).

Because the change of linewidth $\delta\kappa$ depends on the overlap of the antenna and direct cavity radiation, it is expected to depend on the *angular distribution* of both. We therefore study the linewidth change for various cavity modes that are expected to have different field distributions and corresponding radiation profiles, as evidenced by the measurements of Fig. 3. Figure 6 shows the change $\delta\kappa$ of the linewidth on the antenna array compared to that with only a glass substrate, normalized to that on the bare substrate reference (κ_{ref}), for modes with various polar mode numbers *l* within a single mode family. The mode numbers are determined through analysis of the far-field microscopy images (Fig. 3). All measurements are taken at the same cavity-antenna separation. A strong variation of the antenna-induced damping rate is seen, with both increased and decreased cavity linewidth. This provides evidence for the

influence of the cavity radiation profile, which is expected to vary strongly with mode number as the number of nodes along the polar direction increases.

IV. Discussion and conclusions

The above results show that plasmonic nano-antennas can cause both strong frequency shifts and strong changes of the optical linewidth, scaling hundreds of times the intrinsic cavity linewidth of ~3 MHz. In fact, the effects exceed the shift and radiation damping due to a bare substrate of bulk glass with refractive index 1.5, attesting to the large influence of the nanoscale antennas. We have shown that radiative interference of cavity leakage radiation and antenna-induced scattering gives rise to either increased or decreased cavity damping, related to the overlap of both channels. The pronounced effects and controllable coupling strength make this model system ideal to study antenna-cavity interactions in more detail, and unravel the contribution of antenna polarizability, detuning, and radiation properties. Indeed, our setup provides the natural possibility to perform scattering experiments on the antennas in reflection (red arrows in Fig. 2a), providing independent means to study the modes of the nano-antennas as they are altered by the cavity [7], in complementary fashion to the antenna-induced cavity perturbations reported here. Understanding the evolution of the eigenmodes of the coupled system will lead to identification of the possibilities to use hybrid systems for sensing, local field enhancement, and alteration of spontaneous emission probabilities. Finally, it could provide new pathways for strong interactions in cavity optomechanics [18], where changes of both cavity frequency and linewidth [19] can lead to ultrasensitive detection and tailorable optical forces.

References

[1] K. J. Vahala, "Optical microcavities," Nature 424, pp. 839, 2003.

[2] P. Bharadway, B. Deutsch, and L. Novotny, "Optical antennas," Adv. Opt. Photon. 1, pp.438-483, 2009.

[3] E. M. Purcell, "Spontaneous emission probabilities at radio frequencies," Phys. Rev. 69, pp. 681, 1946.

[4] M. Barth, S. Schietinger, S. Fischer, J. Becker, N. Nusse, T. Aichele, B. Lochel, C. Sonnichsen, and O. Benson, "Nanoassembled plasmonic-photonic hybrid cavity for tailored light-matter coupling," Nano Lett. 10, pp. 891, 2010.

[5] F. de Angelis, M. Patrini, G. Das, I. Maksymov, M. Galli, L. Businaro, L. C. Andreani, and E. Di Fabrizio, "A hybrid plasmonic- photonic nanodevice for label-free detection of a few molecules," Nano Lett. 8, pp. 2321, 2008.

[6] M. A. Schmidt, D. Y. Lei, L. Wondraczek, V. Nazabal, and S. A. Maier, "Hybrid nanoparticle-microcavity-based plasmonic nanosensors with improved detection resolution and extended remote-sensing ability," Nature Commun. 3, pp. 1108, 2012.

[7] M. Frimmer and A. F. Koenderink, "Superemitters in hybrid photonic systems: A simple lumping rule for the local density of optical states and its breakdown at the unitary limit," Phys. Rev. B 86, pp. 235428, 2012.

[8] J.-P. Laine, Design and Applications of Optical Microsphere Resonators, PhD thesis, Helsinki University of Technology, 2003.

[9] M. L. Gorodetsky, A. A. Savchenkov, and V. S. Ilchenko, "Ultimate Q of optical microsphere resonators," Opt. Lett. 21, pp. 453, 1996.

[10] L. Novotny, "Effective wavelength scaling for optical antennas," Phys. Rev. Lett. 98, pp. 266802, 2007.

[11] J. Knight, G. Cheung, F. Jacques, and T. Birks, "Phase-matched excitation of whispering-gallery mode resonances by a fiber taper," Opt. Lett. 22, 1129, 1997.

[12] A. N. Oraevsky, "Whispering-gallery waves," Quantum Electon. 32, pp. 377, 2002.

[13] R. A. Waldron, "Perturbation theory of resonant cavities," Poc. Inst. El. Eng., 107C, pp. 272, 1960.

[14] J. S. Schwinger, "The theory of obtacles in resonant cavities and waveguides," MIT Radiation Laboratory Report 43, pp. 34, 1943.

[15] A. F. Koenderink, M. Kafesaki, B. C. Buchler, and V. Sandoghdar, "Controlling the resonance of a photonic crystal microcavity by a near-field probe," Phys. Rev. Lett. 95, pp. 153904, 2005.

[16] M. Burresi, T. Kampfrath, D. van Oosten, J. C. Prangsma, B. S. Song, S. Noda, and L. Kuipers, "Magnetic light-matter interactions in a photonic crystal nanocavity," Phys. Rev. Lett. 105, pp. 123901, 2010.

[17] J. T. Robinson and M. Lipson, "Far-field control of radiation from an individual optical nanocavity: Analogue to an optical dipole," Phys. Rev. Lett. 100, 043902, 2008.

[18] M. Aspelmeyer, T. J. Kippenberg, and F. Marquardt, "Cavity optomechanics," Rev. Mod. Phys. 86, pp. 1391, 2014.

[19] A. Sawadsky, H. Kaufer, R. Moghadas Nia, S. P. Tarabrin, F. Y. Khalili, K. Hammerer, and R. Schnabel, "Observation of generalized optomechanical coupling and cooling on cavity resonance," Phys. Rev. Lett. 114, pp. 043601, 2015.